Molecular view on protein sorting into liquid-ordered membrane domains mediated by gangliosides and lipid anchors

de Jong, Djurre H.; Lopez, Cesar A.; Marrink, Siewert J.

Published in:
Faraday Discussions

DOI:
10.1039/c2fd20086d

Publication date:
2013

Molecular view on protein sorting into liquid-ordered membrane domains mediated by gangliosides and lipid anchors†

Djurre H. de Jong, Cesar A. Lopez and Siewert J. Marrink*

Received 27th April 2012, Accepted 8th June 2012
DOI: 10.1039/c2fd20086d

We present results from coarse grain molecular dynamics simulations of mixed model membranes consisting of saturated and unsaturated lipids together with cholesterol, in which lipid-anchored membrane proteins are embedded. The membrane proteins studied are the peripherally bound H-Ras, N-Ras, and Hedgehog, and the transmembrane peptides WALP and LAT. We provide a molecular view on how the presence and nature of these lipid anchors affects partitioning of the proteins between liquid-ordered and liquid-disordered domains. In addition, we probed the role of the ganglioside lipid GM1 on the protein sorting, showing formation of GM1-protein nano-domains that act as shuttles between the differently ordered membrane regions.

1 Introduction

The organisational principles of the cell membrane are amongst the great open questions in biology.[1–3] The cell membrane (or plasma membrane) consists of a mixture of different lipids, transmembrane proteins and membrane anchored soluble proteins. In order to bring together functional components in such a complex mixture the plasma membrane is believed to be compartmentalized, thus restricting the conformational search problem. These membrane compartments, or domains are typically known as lipid rafts[4] and are enriched in sphingolipids, cholesterol and specific proteins. The current view describes these rafts *in vivo* as nanoscale assemblies that may condense into larger platforms under relevant conditions.[2] *In vitro*, the segregation of ternary lipid mixtures into a liquid ordered (Lo) and liquid disordered (Ld) membrane is considered to be a good model for membrane compartmentalization.[5–7] In such model systems, transmembrane proteins are typically found segregated into the Ld phase, even in the case of raft-associated proteins. This leaves us with a fundamental question how cells are able to regulate protein sorting into more ordered regions of the membrane.

In order to target proteins towards rafts, lipids are believed to play an important role. The lipid–protein interaction could be chemically enforced, *i.e. via* lipid anchors, or occur through either specific or non-specific binding. Different types of lipid anchors include glycophosphatidylinositol (GPI), palmitoyl, isoprenyl or sterol anchors, and are found for both peripheral and transmembrane proteins.[8] These anchors have a natural affinity for the raft domains and may drag the protein along. Binding of proteins to raft lipids could be another mechanism by which proteins are being sorted. Specific lipid binding sites are found, for example, for

Nijenborgh 7, 9747AG Groningen, The Netherlands. E-mail: s.j.marrink@rug.nl; Fax: +31 50 363 4398; Tel: +31 50 363 4457

† Electronic Supplementary Information (ESI) available: Detailed parameterization procedure for GM1 lipids. See DOI: 10.1039/c2fd20086/

the p24 transmembrane protein recognizing certain sphingolipids[9] or the influenza virus M2 protein binding cholesterol.[10] Besides sphingolipids and cholesterol, ganglioside lipids are an important component of rafts.[11–15] Gangliosides are ceramide based lipids with an oligosaccharide head group. GM1 and GM3, two well known ganglioside lipid species, bind different proteins (both soluble[16,17] and transmembrane[18,19]) and promote formation of extended raft domains upon cross-linking with antibodies.[20]

Despite the vast amount of research effort in the last decade, the underlying organising principles of cell membranes are not yet fully understood. To gain molecular insight in the driving forces of membrane protein segregation, coarse grain (CG) molecular dynamics simulations are a promising technique.[21–24] The CG Martini model[25,26] has proven to work well in this respect. Applying the Martini model, we recently were able to correctly predict the partitioning of transmembrane (TM) helices between domains in Lo–Ld phase separated model membranes consisting of ternary mixtures of saturated lipids, unsaturated lipids, and cholesterol.[27,28] These simulations allowed us to evaluate the underlying mechanism by which small proteins are sorted into the Ld phase. The driving force for partitioning into the Ld phase was shown to originate from lipid packing effects.

Here we extend these studies in order to investigate the role of lipid anchors in steering the sorting of membrane proteins. The proteins considered are the peripheral proteins H-Ras and N-Ras, which have a farnesyl anchor together with two or one palmitoyl anchors, respectively, and Hedgehog, a cholesterol anchored peripheral protein. We also studied the TM peptides WALP and linker for activation of T-cells (LAT) with two palmitoyl anchors attached. Additionally, we simulated the ability of small amounts of GM1 gangliosides to affect the sorting process in case of the TM peptides.

2 Methods

2.1 System setup

All systems are based upon a spontaneously demixed bilayer consisting of 828 dipalmitoyl-phosphatidylcholine (diC(16 : 0)PC, DPPC), 540 dilinoeoyl-phosphatidylcholine (diC(18 : 2)PC, DLiPC), and 144 cholesterol CG molecules, solvated by 12 600 CG water beads representing 50 400 real waters. The simulation cell measures approximately 21.7 by 21.7 nm in the lateral (x,y) dimensions and 7.5 nm in the perpendicular z-direction. Domanski *et al.*[28] found this mixture to be weakly phase separating into Ld and Lo domains with a line tension of 2 ± 2 pN. Additionally, the systems contained either four copies of anchored peripheral proteins (H-Ras, N-Ras, or Hedgehog) or twelve lipid anchored transmembrane peptides (WALP23 or LAT). In some systems 32 ganglioside lipids (GM1) were added. An overview of the systems simulated is given in Table 1, and a graphical overview of the membrane constituents is shown in Fig. 1.

In systems containing the anchored peripheral proteins H-Ras, N-Ras, or Hedgehog, the four proteins were initially positioned on a regular grid. The globular domains were put approximately 2 nm above the membrane, all on the same face of the membrane. To accommodate the lipid anchors, one of the membrane lipids was replaced by either one (N-Ras) or two (H-Ras) of the palmitoyl anchors (effectively lowering the amount of lipids in a monolayer by $\sim$1% for the four proteins in total). The farnesyl tail was inserted in the membrane separately. For Hedgehog, a membrane cholesterol was substituted. The system size in the z-direction was enlarged by 6 nm to ensure that periodic images would not interact and subsequently 24 043 additional water beads were added to solvate the system. In the case of the Ras proteins, 24 sodium counter ions were added to neutralize the system, equivalent to four times the minus 6 charge of a single protein.

Table 1 Overview of simulated bilayer systems

System	Composition	Simulation time (μs)	Number of simulations
Reference			
A	DPPC : DLiPC : Chol (828 : 540 : 144)	10	1
Peripheral proteins			
B	A + 4 H-Ras	12	1
C	A + 4 H-Ras (no Pal.)	12	1
D	A + 4 N-Ras	12	1
E	A + 4 Hedgehog	12	1
Transmembrane peptides			
F	A + 12 WALP	12	1
G	A + 12 WALP (no Pal.)	12	1
H	A + 12 LAT	10	1
Gangliosides			
I	A + 4% GM1	12	1
J	F + 4% GM1	10	2
K	H + 4% GM1	10	2

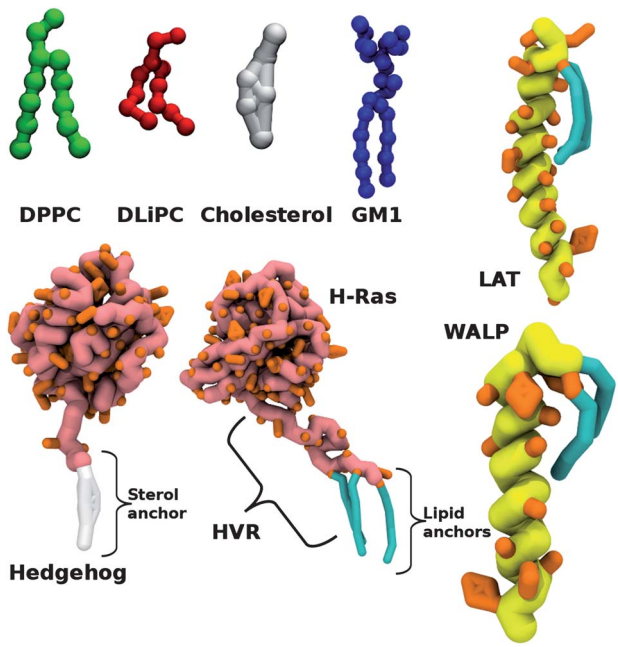

Fig. 1 Coarse grain representation of membrane constituents considered in this work. The Martini model is used, which maps on average four heavy atoms into a single CG bead. Secondary structure of the proteins is constraint in this model. Molecules are depicted at different scales. The colour scheme is corresponding to the one used in the remaining figures. The N-Ras protein is similar to H-Ras, but lacks one of the palmitoyl anchors. HVR stands for hyper variable region, an unstructured part of the Ras protein.

For the systems containing LAT-peptides, 12 peptides were inserted in a parallel manner on a regular grid. The parallel orientation is consistent with *in vivo* systems where membrane proteins are oriented with positively charged residues towards the

cytoplasm, the so called 'positive inside rule'.[29] The WALP peptides were inserted in a similar manner, except they were positioned in an alternating parallel–antiparallel fashion, mimicking the random 'up–down' orientation found in experiments.[30] Both LAT and WALP peptides were initially placed overlapping with the membrane, and overlap was subsequently removed by energy minimization (see below). Addition of 12 sodium counter ions assured neutralizing the charge of the 12 LAT peptides.

In systems containing GM1 lipids, 16 lipids were added to both monolayers, equivalent to ~4 mol% lipids. The GM1 lipids were initially positioned on a regular grid. In systems containing both peptides and GM1 lipids the peptide and ganglioside grids were shifted with respect to each other, in order to have no initial overlap between the GM1 lipids and peptides. One additional sodium ion per GM1 lipid was added as a counter ion.

2.2 Molecular parameters

The Martini CG forcefield[25,26] was used for all systems. The parameters for DPPC, DLiPC and cholesterol, as well as those of water and ions, can be found in previous publications.[25,31] The CG representation of all membrane constituents is shown in Fig. 1. All parameters used in this study can be downloaded from http://cgmartini.nl.

For H-Ras and N-Ras, structures were taken from the PDB-database (121P[32] & 3CON[33]). H-Ras is crystallized in its activated state, bound to the GTP mimicking inhibitor GCP, and N-Ras is crystallized in its inactive state, bound to GDP. The soluble domain is connected to the membrane *via* lipid anchors that reside in an unstructured stretch of amino acids known as the hyper variable region, HVR (*cf.* Fig. 1). The C-terminal HVR, residues 166–186, was modelled as a random coil using Pymol.[34] The missing residues in the structure of N-Ras were modelled based upon homology to H-Ras. The complete protein was converted to CG based on the Martini protein force field[26] and using the martinize-script.[35] Ligands were left out and the ternary structure was kept stable using an elastic network.[36] The Cα root mean square deviation (RMSD) of the soluble protein domain (excluding the flexible HVR) never exceeds 0.3 nm for both H-Ras and N-Ras due to the elastic network. Palmitoyl anchors, using the standard Martini mapping[25] for palmitoyl chains (Na–C1–C1–C1–C1), were connected to cysteine 181 and 184 (H-Ras) or 184 (N-Ras) side chains using a harmonic bond with equilibrium distance $r_0 = 0.39$ nm and force constant $f_c = 5000$ kJ mol^{-1} nm^{-2}. The C-terminal cysteine residue 186 was farnesilated. Our model of the farnesyl tail consisted of a linear sequence of three C3 beads, all connected *via* harmonic bonds with $r_0 = 0.49$ nm and $f_c = 8000$ kJ mol^{-1} nm^{-2}. The angle bending is restricted by harmonic potentials with a 140° equilibrium angle and $f_c = 200$ kJ mol^{-1}. The first C3 bead was connected to the cysteine side chain bead using a harmonic bond with $r_0 = 0.39$ nm, $f_c = 5000$ kJ mol^{-1} nm^{-2}.

The Hedgehog protein structure was taken from the PDB-database (1VHH[37]). The three missing residues (Ser196, Gly197, Gly198) were modelled as a random coil. The atomistic structure was converted to CG based on the Martini protein force field[26] and using the martinize-script.[35] For the cholesterol anchor the standard Martini cholesterol parameters[25] were used. The hydroxyl bead of the cholesterol was connected to the C-terminal glycine residue by a harmonic bond with $r_0 = 0.35$ nm, $f_c = 400$ kJ mol^{-1} nm^{-2}.

Topologies for the WALP23 (GW_2L-$(AL)_8$-W_2A) peptides[38] were also generated using the Martini protein parameters,[26] thus constraining the α-helicity for the whole peptide. A glutamic acid is connected to the N-terminal glycine *via* a succimide moiety.[39] This reverses the N-to-C terminus direction of the glutamic acid backbone, thus creating two carboxylic acid groups, one on the side chain and one on the backbone C-terminus. Palmitoyl anchors are connected to both carboxylic acids (see Fig. 1). Succinimide is modelled as a polar P5 particle and connected to the glycine and glutamate backbone beads by relatively weak harmonic bonds with $r_0 = 0.47$ nm, $f_c = 200$ kJ mol^{-1} nm^{-2}. The palmitoyl tails are connected to the glutamate

backbone and side chain bead by a harmonic bond with $r_0 = 0.34$ nm, and $f_c = 1250$ kJ mol^{-1} nm^{-2}. No angle or dihedral potentials involving either the succinimide or glutamate beads were defined.

The LAT peptide (EADWLSPVGLGLLLLPFLVTLLAALCVRCRE, residues 2–32 of Murine LAT, with substitution Trp for Ala[4]) was modelled in a similar way as the WALP peptide. Palmitoyl anchors were connected to both cysteine residues' side chains using harmonic bonds with $r_0 = 0.39$ nm, $f_c = 5000$ kJ mol^{-1} nm^{-2}.

The GM1 ganglioside lipids were parameterized based upon the extension of the Martini model towards carbohydrates.[40] A detailed description of the parameterization of GM1 is given in the ESI.†

2.3 Simulation parameters

All systems were simulated using the Gromacs MD package[41] (version 4.5.3). After minimizing the system energy by 500 steps steepest descent, the systems were simulated using a leap-frog integrator with a time step of 20 fs. A constant particle number, pressure and temperature (NpT) ensemble was applied. Pressure in the lateral (xy) and normal (z) dimensions was coupled separately to a 1 bar external bath with coupling time constant, $\tau_p = 3.0$ ps and compressibility, $\chi = 3.0 \times 10^{-5}$ bar^{-1}. Temperature is kept constant at 295 K by coupling to an external temperature bath with a coupling time constant, $\tau_t = 1.0$ ps. Three groups of molecules were coupled separately to avoid heat flow: water and ions, lipids and proteins, and cholesterol. Most systems were run for more than 10 μs, see Table 1 for total simulation times. Note that we report actual simulation times; due to the smoothing of the potential energy surface in CG models, the effective time is longer. For lipids and proteins in the Martini model, the speed-up factor is about fourfold,[42] *i.e.* 10 μs simulation time would correspond to 40 μs real time.

2.4 Analysis

The preferential partitioning of membrane components is calculated as the relative number of contacts of a lipid species with each of the other lipid constituents, corrected for the total number of lipids in the system:

$$p_A = \frac{c_A/n_A}{\sum_\chi c_\chi/n_\chi} \quad (1)$$

where p_A is the preferential partitioning with membrane component A, c_A the number of contacts with component A and n_A the number of molecules of component A. Using this formula random mixing would give an equal preferential partitioning with all components (*e.g.* 0.50 for a two component comparison). Note that eqn. (1) does not take into account the number of contacts per molecule of the different membrane constituents. Since in this work we only compare lipids of equivalent size, this effect will be negligible. Contacts were defined with respect to the GL1 and GL2 beads for lipids, all anchor beads for the soluble proteins and either the peptide with the anchor or just the anchor for the TM peptides. Two molecules were counted 'in contact' if they were within 1.1 nm, roughly corresponding to the second solvation shell. The second solvation shell was chosen to obtain better statistics. Using only the first solvation shell (<0.8 nm) gave comparable results. The Gromacs analysis tool g_mindist was used to calculate the number of contacts, analysing a trajectory frame every 1 ns. The first part of each of the simulations was omitted as the equilibration phase. The system was considered equilibrated if the number of DPPC–DPPC contacts became constant, typically requiring between 2 and 5 μs. Comparing the number of contacts between various components showed the number of DPPC–DPPC contacts to be in general a good indicator for the state of equilibration of the system.

Density profiles were calculated by first centering the bilayer in the box, based upon the last tail bead of all lipids over the course of the simulation. Subsequently the number density profiles were calculated using the Gromacs analysis tool g_density and normalized afterwards.

3 Results and discussion

We study the preferential partitioning of several bilayer constituents in a phase separated model membrane. Our reference system (*mixture A*) is a weakly phase separated membrane containing DPPC, DLiPC, and cholesterol in a 828 : 540 : 144 molar ratio, approximating 6 : 4 : 1. It consists of a liquid ordered (Lo) domain enriched in DPPC and cholesterol and a liquid disordered (Ld) domain enriched in DLiPC. The highly dynamic domain behaviour and a line tension of 2 ± 2 pN of this system resemble the characteristics of *in vivo* systems[2,20] and thus our system is very suitable to study the preferential partitioning of different bilayer constituents.

The remainder of the results section is split into three parts. First, we describe simulations of the partitioning of peripheral proteins, which are anchored to the membrane by either palmitoyl and farnesyl anchors or a cholesterol anchor. Next we consider single helix transmembrane peptides, with two palmitoyl anchors. Finally, we look at the partitioning behaviour of gangliosides and their ability to influence the partitioning of membrane lipids and transmembrane peptides. Table 1 gives an overview of the contents and total simulation time of the simulated systems. To quantify the preferential partitioning we calculated the normalized number of contacts with DPPC and DLiPC lipids. We compare against DPPC and DLiPC as they are the main constituents of the Lo and Ld phase, respectively, and serve as a marker for these phases.

3.1 Partitioning of peripheral proteins into the Lo domain mediated by lipid anchors

To investigate the partitioning of membrane anchored soluble proteins we added four copies of a Ras protein to the reference mixture. The Ras proteins are peripheral membrane proteins belonging to the family of GTPases and are involved in signal transduction pathways that control cell growth and proliferation.[43] Here we study both N-Ras and H-Ras (*mixtures B and D*), which have a high sequence identity (>90%) over the 165 N-terminal residues (G-domain) and much lower sequence identity (10–15%) in the C-terminal[24] residues forming the HVR.[44] The membrane anchors are found in the HVR, and consist of a farnesyl tail at the terminal cysteine residue (Cys 186), and either one or two palmitoyl chains in N-Ras (Cys 181) and H-Ras (Cys 181 and 184), respectively,[44] see Fig. 1. We also simulated a system containing de-palmitoylated H-Ras (*mixture C*), *i.e.* H-Ras with one farnesyl but no palmitoyl tails.

Starting from a regular distribution over the membrane, the three different Ras proteins show distinct behavior. H-Ras is observed to partition into the Lo phase over a time scale of several μs, whereas N-Ras and de-palmitoylated H-Ras have a preference for the Ld phase, as shown in Fig. 2. The soluble G-domains form an aggregate within 5 μs of simulation time for all three proteins. Once the cluster has formed only minor reorientations of the monomers with respect to each other are observed. Table 2 shows the normalized number of contacts of the Ras proteins with DPPC and DLiPC. The addition of the anchored protein does not affect the (de)mixing of the DPPC and DLiPC lipids as visible from the normalized number of contacts which stay close to the corresponding values in the reference system. The H-Ras protein anchors have more contacts with the DPPC lipids, in other words they preferentially partition to the Lo phase consistent with the images shown in Fig. 2. N-Ras and de-palmitoylated H-Ras have more contacts with DLiPC, most pronounced for the latter. Especially N-Ras can be considered as line-active, *i.e.* spending most time at the border between Lo and Ld domains (bottom row Fig. 2).

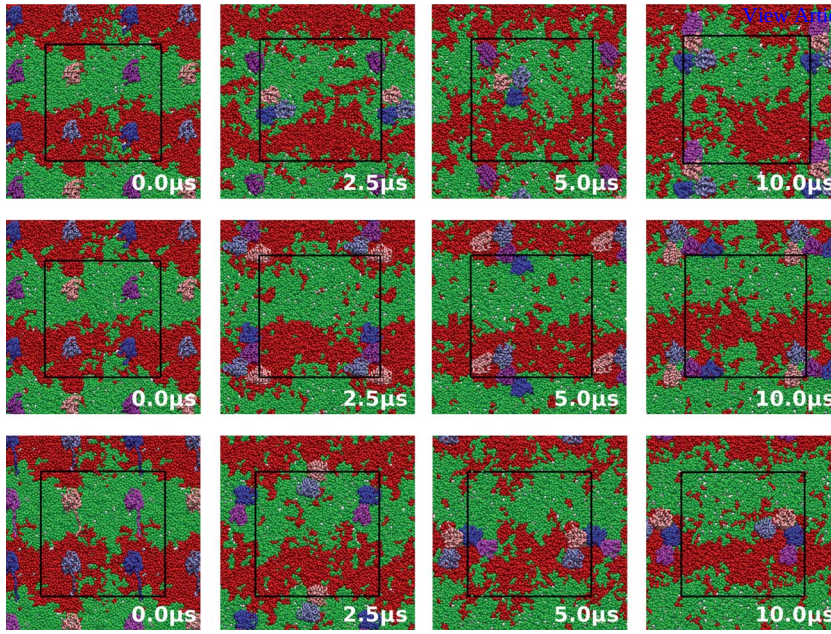

Fig. 2 Anchor driven partitioning of Ras proteins into membrane domains. Top view snapshots from a simulation of four copies of the H-Ras (top), de-palmitoylated H-Ras (middle) and N-Ras (bottom) peripheral proteins in a DPPC : DLiPC : cholesterol lipid mixture. The different copies of the proteins are coloured pink, purple, blue and light blue. DPPC, DLiPC and cholesterol are coloured red, green and white, respectively. The black line shows the simulation box.

Table 2 Normalized number of contacts p_A of bilayer systems containing peripheral proteins[a]

	Reference		H-Ras		N-Ras		H-Ras (no Pal.)		Hedgehog	
	DPPC	DLiPC	DPPC	DLiPC	DPPC	DLiPC	DPPC	DLiPC	DPPC	DLiPC
DPPC	0.79	0.21	0.78	0.22	0.78	0.22	0.79	0.21	0.80	0.20
DLiPC	0.19	0.81	0.20	0.80	0.20	0.80	0.19	0.81	0.18	0.82
Anchor			0.68	0.32	0.41	0.59	0.22	0.78	0.74	0.26

[a] The values for a system in one row are normalized (add up to one). Errors in p_A, based on block-averaging and assuming independent blocks over 500 ns, are of the order of 0.03.

Our data on partitioning of Ras proteins are in agreement with recent *in vitro* studies, showing a preference for N-Ras to accumulate at the domain boundaries.[45] K-Ras, which only has a farnesyl anchor in addition to a polybasic membrane unit, is found[46] to partition into the Ld domain consistent with our results for de-palmitoylated H-Ras. Recent results from CG simulations by Janosi *et al.*[47] who studied the partitioning of the isolated Ras anchors, are consistent with our data, and confirm the antagonistic action of farnesyl and palmitoyl tails.

Interestingly, *in vivo* data[48,49] show the partitioning of H-Ras to either the raft or non-raft phase to be regulated by additional factors. In particular, GTP loading (*i.e.* activation) segregates H-Ras from the raft phase to the non-raft phase while the GDP bound form (*i.e.* inactive) segregates to the Lo domain. This different behaviour upon GTP binding is hypothesized to be caused by a structural change of the

soluble N-terminal domain, coupling to a different orientation or conformation of the HVR to which the anchors are attached.[50] A change in membrane insertion of the Lo phase preferring, palmitoyl anchors *versus* the, Ld phase preferring, farnesyl anchors could thus be achieved, changing the relative propensity for either phase. Our observation that the GCP bound (activated) H-Ras partitions to the Lo phase appears in contradiction with this. Apparently, in our simulations, the driving force provided by the lipid anchors is insufficiently modulated by the structural differences due to activation or deactivation. This might be explained by several factors: first, the H-Ras structure used here was determined using GCP as a (inhibiting) ligand instead of the natural GTP. Possible small structural changes as a result of this might influence the partitioning behaviour. Second, the HVR region is modelled as a random coil, which might be inappropriate for the activated state of Ras. Third, the relative partitioning of the palmitoyl *versus* farnesyl anchors might depend on the overall lipid composition of the membrane.

To study the role of the lipid anchors and the HVR in more detail, we characterized the lateral position of the lipid anchors and fluctuations of the HVR region. For the anchors we analyzed their particle density along the bilayer normal. The result is shown in Fig. 3 together with a graphical snapshot of the final configuration of the systems. When comparing the position of the last tail bead of the membrane lipids, it can be seen that the palmitoyl and farnesyl anchors are not inserted as deeply into the bilayer as DPPC lipids. This is true for both H-Ras and N-Ras. In other words the attachment of lipid anchors to the protein backbone slightly pulls the anchors out of the membrane. The farnesyl tail is inserted less deeply into the membrane compared to the palmitoyl anchors which can be attributed to the shorter length of the farnesyl unit. In all-atom simulations, Gorfe *et al.*[50] found the farnesyl tail of H-Ras to be inserted deeper into the membrane as compared to the palmitoyl

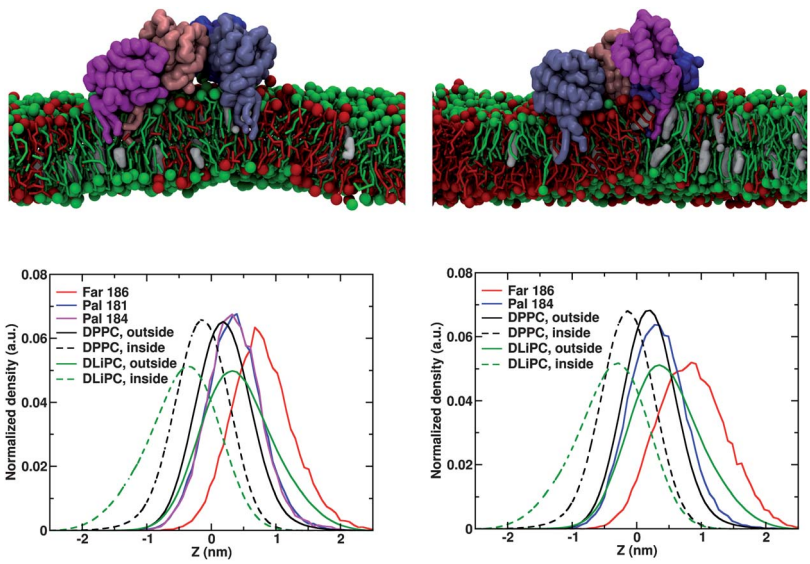

Fig. 3 Positioning of palmitoyl and farnesyl anchors of Ras proteins inside the membrane. Top: sideview of the H-Ras (left) and N-Ras (right) protein complexes after 10 μs. The different copies of the proteins are coloured pink, purple, blue and light blue. DPPC, DLiPC and cholesterol are coloured red, green and white, respectively. Bottom: Normalized density profiles along the *z*-axis for H-Ras (left) and N-Ras (right) lipid anchors. Density profiles are plotted for the last tail beads of the farnesyl (red) and palmitoyl (blue and pink) anchors and DPPC (black) and DLiPC (green) lipids. Solid and dashed lines indicate the inner and outer monolayer, respectively.

tails, however in their model the farnesyl tail is modelled by a longer (saturated) hexadecyl unit, which affects the membrane insertion. The HVR does not adopt a stable, well defined structure, comparable to the work of Gorfe *et al.*[50] and experimental results.[51] The fluctuations, measured by the pairwise RMSD (mean: 0.14, 0.13 and 0.18 nm for H-Ras, de-palmitoylated H-Ras and N-Ras, respectively), are similar to those reported by Gorfe *et al.*[50] for the HVR with G-domain connected.

A much less abundant membrane anchoring mechanism is *via* the attachment of a sterol moiety, found in the Hedgehog protein family.[52] Although the complete form of the human Hedgehog protein is both C-terminally sterolated and N-terminally palmitoylated,[53] it was found that the C-terminal sterol anchor is sufficient for the protein to partition to detergent-resistant membrane patches.[54] Here we study the partitioning of the C-terminally sterol anchored Hedgehog protein, by placing four protein copies in the reference mixture (*mixture E*, Table 1). Similar to palmitoyl anchors of the Ras proteins, also the cholesterol anchor is able to drive the peripheral protein into the Lo domain. Fig. 4 shows the final snapshots from the simulation, with the Hedgehog protein clearly residing in the Lo domain. Once in the Lo phase the proteins form a cluster and never enter the Ld phase again.

Analysis of the normalized number of contacts of the four cholesterol anchored Hedgehog proteins with the other membrane components, shown in Table 2, underlines the strong preference for saturated lipids. Partitioning of cholesterol-anchored Hedgehog into the Lo phase is in agreement with the experimentally known behaviour[54]

Together, our data on peripheral membrane proteins show that lipid anchors provide a strong driving mechanism for selective partitioning. The anchors considered, either palmitoyl or sterol anchors, show a strong preference for the Lo phase in line with expectations. The ability of the farnesyl anchor of the Ras proteins to provide a counter force toward the Ld phase is also apparent from our simulations.

3.2 Lipid anchors also modulate partitioning behaviour of TM peptides

Both the synthetic WALP transmembrane peptide and the linker for activation of T-cells (LAT) have been extensively studied with respect to domain partitioning. WALP peptides were specifically designed to study the behaviour of TM proteins in lipid bilayers[55] and have been shown to partition into the Ld phase in model membranes, both with[39] and without[27] palmitoyl anchors. Palmitoylated LAT has been both reported to partition to the Lo and Ld domain, depending on the method of preparation of the membrane system. In synthetically devised lipid mixtures

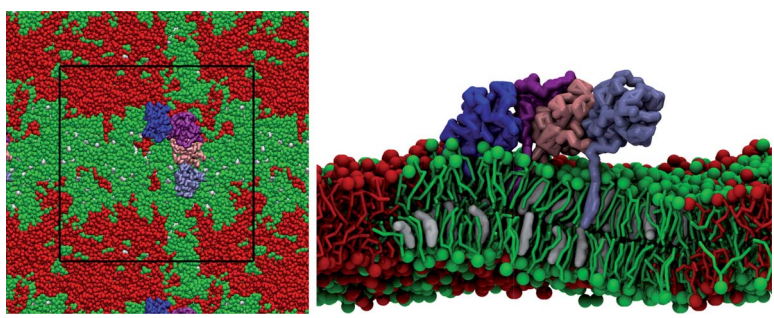

Fig. 4 Anchor driven partitioning of Hedgehog proteins into the Lo domain. Top (left) and side (right) view of a simulation of 4 Hedgehog peripheral proteins in a DPPC : DLiPC : cholesterol lipid mixture after 12 μs. The different copies of the proteins are coloured pink, purple, blue and light blue. DPPC, DLiPC and cholesterol are coloured red, green and white, respectively. The black line shows the simulation box.

palmitoylated LAT prefers the Ld phase,[56] whereas in plasma membrane spheres obtained from real cells, it prefers the Lo domain.[57] It has been hypothesized that this contrasting behaviour in the differently prepared membranes systems can be attributed to a degree of order difference between the Lo and the Ld phase[20] in the two systems. To study the behaviour of these lipid anchored TM peptides, we added either 12 WALP23 or 12 LAT peptides with two palmitoyl chains each to the reference mixture (*mixtures F*,*H*, Table 1). For comparison, a system containing WALP without palmitoyl anchors was also simulated (*mixture G*).

Fig. 5 shows snapshots from these simulations. Both LAT and WALP peptides are segregated out of the bulk of the Lo phase within 1 μs. Once the peptides have segregated from the Lo phase, they show very different behaviour. For the WALP peptides the behaviour is very dynamic. First, they form peptide–peptide clusters that constantly form and break up again, consistent with earlier observations.[27] Monomers, dimers and trimers are observed throughout the simulation. Second, the WALP peptides do not remain in the bulk of the Ld phase but often reside close to the domain boundary and in transiently formed lipid peninsulas or lipid islands. The addition of the transmembrane peptides does not notably change the mixing of the lipids (Table 3). The normalized number of contacts indicates a strong preference of the WALP peptide for the Ld phase, but not as strong as in the case of WALP without anchors. To study the orientation of the peptides we calculated the number of contacts of the anchor to DPPC and DLiPC. The preference for the Ld phase remains, although less strong, indicative of an orientation, and consecutive dragging force, of the (saturated) lipid anchors towards the Lo phase. In experiments[39] on artificial lipid mixtures, single or double palmitoylation is not sufficient to bring WALP into the Lo phase, matching our current results.

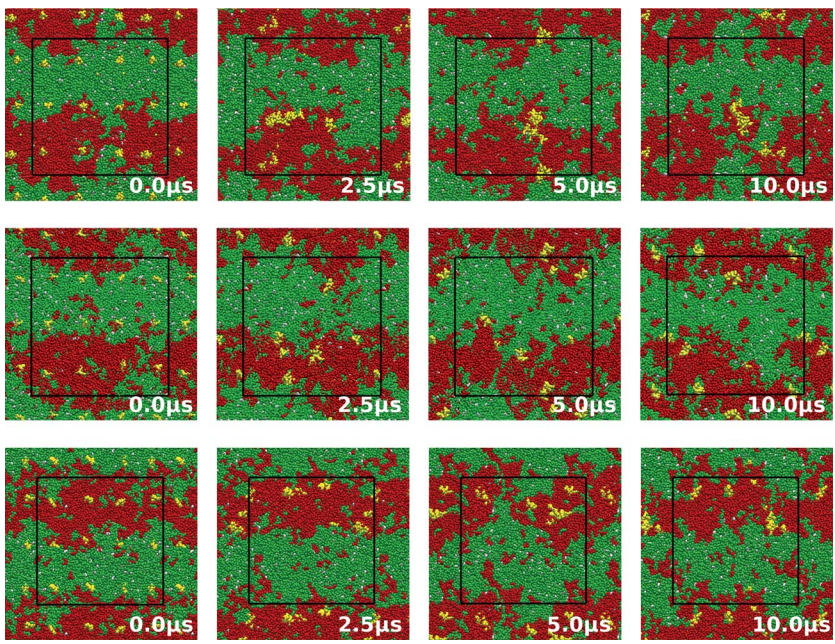

Fig. 5 Anchor driven partitioning of TM peptides toward the Lo–Ld phase boundary. Top view of bilayer systems containing 12 LAT peptides (top) or 12 WALP peptides (middle) with anchors and 12 WALP peptides without anchors (bottom). Green is the saturated DPPC lipids, red the unsaturated DLiPC lipids, white is cholesterol, and yellow the TM peptides.

Table 3 Normalized number of contacts p_A of bilayer systems containing TM peptides[a]

	Reference		WALP		LAT		WALP (no Pal.)	
	DPPC	DLiPC	DPPC	DLiPC	DPPC	DLiPC	DPPC	DLiPC
DPPC	0.79	0.21	0.80	0.20	0.79	0.21	0.80	0.20
DLiPC	0.19	0.81	0.19	0.81	0.19	0.81	0.19	0.81
Anchor			0.40	0.60	0.67	0.33		
Peptide			0.22	0.78	0.27	0.73	0.09	0.91

[a] The values for a system in one row are normalized (add up to one). Errors in p_A, based on block-averaging and assuming independent blocks over 500 ns, are of the order of 0.03.

In contrast to WALP, the LAT peptides form a constantly growing cluster: once a peptide binds to a partner, they never break up again (Fig. 5). The lipid anchors of the clustered peptides are oriented towards the same side of the cluster and towards the Lo domain, but the peptides still reside in the Ld domain. This leads to a higher normalized number of contacts of the anchors to DPPC compared to the combination of peptides and anchors (Table 3). The LAT peptides show a slightly higher normalized number of contacts to DPPC lipids compared to WALP, but the preferred contact is with the unsaturated lipids found in the Ld region. The partitioning of palmitoylated LAT into the Ld phase agrees with the experimental results using artificial membranes,[56] and not those in plasma membrane spheres.[57] This indicates that the difference in order between the Lo and Ld domains in the current mixture is larger than that of real membranes, assuming that the plasma spheres more closely resemble the *in vivo* situation.

We conclude that the palmitoylation of TM peptides indeed provides a driving force toward the more ordered membrane domains. Two saturated lipid anchors, however, are not sufficient to allow the peptides to dissolve into the Lo domains. The orientation of the lipid anchors towards the Lo domains endorses the important role of lipid anchors; in fact the anchored peptides show linactant behaviour,[58] residing most of the time at the domain boundaries.

3.3 Gangliosides are able to shuttle proteins into the Lo phase

Ganglioside lipids are strongly amphiphilic lipids due to their large carbohydrate head group and their ceramide based lipid tails. They are enriched in detergent resistant membrane domains and are thought to play an important role in the formation of those domains.[12,13,20] Here we investigate the effect of GM1 gangliosides (see Fig. 1) on membrane domain formation and their interaction with TM peptides. We first looked at the partitioning of GM1 lipids between the Lo and Ld domains of our ternary lipid system. In order to do so we added 4 mol% GM1 lipids to our reference mixture (*mixture I*).

The top row of Fig. 6 illustrates the time evolution of this system. Placed initially on a homogeneous grid, the GM1 lipids are observed to aggregate into a single domain in about 10 μs. These nano-domains are registered over both monolayers and are dynamic, *i.e.*, the gangliosides remain in a fluid state. To quantify the extent of mixing in this quarternary membrane mixture, the normalized number of contacts of the different system components with respect to DPPC (Lo) and DLiPC (Ld) were calculated. The data are gathered in Table 4, from which a number of conclusions can be drawn. First, the extent of demixing of DPPC and DLiPC does not change significantly upon addition of the small amount of GM1 (compare to reference mixture in Table 2). Second, GM1 shows a very strong preference for DPPC lipids over DLiPC lipids, implying GM1 associates with the Lo lipids; this is also evident

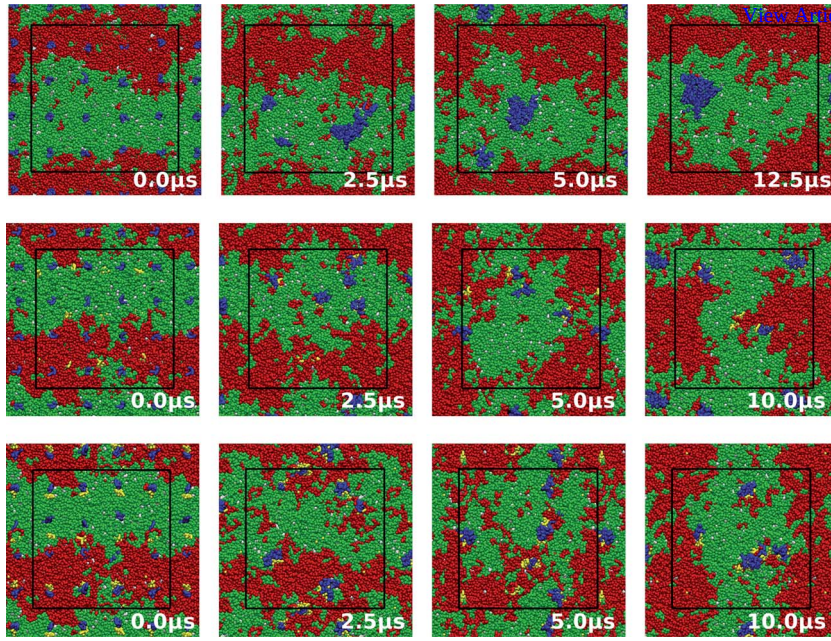

Fig. 6 Ganglioside mediated shuttling of TM peptides toward the Lo domains. Top view of bilayer systems containing 4 mol% GM1 lipids (top), 4 mol% GM1 and 12 WALP peptides (middle) or 4 mol% GM1 and 12 LAT peptides (bottom). Green is used to depict the saturated DPPC lipids, red the unsaturated DLiPC lipids, white the cholesterols, blue the GM1 and yellow the TM peptides.

from the snapshots in Fig. 6. Third, when preferential partitioning parameters are calculated with respect to three groups, DPPC, DLiPC and GM1, GM1 shows the strongest preference for self-association, consistent with the formation of a nano-domain. Finally, the number of contacts for cholesterol indicates an enrichment of the GM1 domain in cholesterol with respect to the surrounding Lo domain.

Experimental data on the phase behaviour of GM1 containing membranes are limited (see recent reviews[12,13]). Besides, interpretation of these data is not straightforward due to the fact that GM1 lipids can have either saturated and unsaturated tails next to the sphingosine moiety. In our simulations, we use a fully saturated tail. Experimentally, fully saturated GM1 shows a high affinity for Lo phases, in line with our results. Moreover, there is growing evidence[12,13] that GM1 can form laterally separated Lo nano-domains, and this corroborates our findings. Based on measurements on mixtures of GM1, sphingomyelin (SM), and cholesterol, a depletion of cholesterol from the ganglioside domain was concluded.[59] This is in contrast to our observation, which indicates a small but significant cholesterol enrichment of the GM1 domain. The difference might be explained by the difference in lipid mixtures. SM lipids are known to have a higher affinity for cholesterol than DPPC lipids do, therefore cholesterol depletion of GM1 domains is expected with respect to SM but not DPPC. Realizing that GM1 lipids also have a ceramide backbone, the condensation of GM1 and cholesterol into a single domain seems rather plausible.

Next we address the question to which extent GM1 can have an effect on the partitioning of TM peptides. To do so, we added 4 mol% GM1 to the membranes containing 12 doubly palmitoylated WALP or LAT peptides (*mixtures J*,*K*, Table 1). Snapshots from these simulations are shown in Fig. 6, together with the GM1 containing membrane without peptides discussed above. Initially, the peptides and

Table 4 Normalized number of contacts p_A of lipids in GM1 containing bilayers[a]

	No Peptide					WALP					LAT				
	DPPC	DLiPC	DPPC	DLiPC	GM1	DPPC	DLiPC	DPPC	DLiPC	GM1	DPPC	DLiPC	DPPC	DLiPC	GM1
DPPC	0.78	0.22	0.49	0.14	0.37	0.78	0.22	0.57	0.16	0.27	0.77	0.23	0.54	0.17	0.29
DLiPC	0.19	0.81	0.18	0.78	0.04	0.20	0.80	0.17	0.68	0.15	0.21	0.79	0.19	0.68	0.13
GM1	0.94	0.06	0.06	0.0	0.94	0.66	0.34	0.07	0.03	0.90	0.69	0.31	0.06	0.03	0.91
Cholesterol			0.30	0.05	0.65			0.50	0.09	0.41			0.39	0.09	0.52
Peptide						0.44	0.56	0.05	0.05	0.90	0.34	0.66	0.03	0.07	0.90
Anchor						0.65	0.35	0.05	0.05	0.90	0.61	0.39	0.07	0.04	0.90

[a] The values for a system in one row are normalized (add up to one). Errors in p_A, based on block-averaging and assuming independent blocks over 500 ns (no peptide) or based on the differences between two simulations (WALP and LAT) are of the order of 0.03.

GM1 lipids were added on overlapping grids. Due to the larger number of GM1 lipids (16) compared to peptides (12), this placement results in some close peptide–GM1 contacts right from the beginning, as well as some isolated peptides and gangliosides. Within a few μs, however, almost all of the peptides and GM1 lipids are binding to each other, forming small, mixed clusters which merge to form larger clusters. The mixtures with WALP or LAT peptides show comparable behaviour. At the end of the simulations, no clusters containing only GM1 lipids or TM peptides are observed. It is likely that the simulations have not yet reached equilibrium at this stage, and that eventually the few remaining clusters at 10 μs will coalesce into one nano-domain. In contrast to the GM1 clusters in the systems containing no peptides, the clusters are depleted of cholesterol (with respect to the Lo domain), but do contain DLiPC, as can be inferred from the increased normalized number of contacts for GM1 and cholesterol with the other constituents (Table 4). Closer inspection of the organization of the GM1–peptide clusters reveals a tendency to remain at the Lo–Ld domain boundary, which explains the apparent substitution of cholesterol for unsaturated lipids. The presence of the GM1–peptide clusters also leads to slightly more mixing of DPPC and DLiPC, which again would point to linactant behaviour. Comparing systems that contain 4 mol% GM1 to systems without GM1 (*cf.* Table 2 and 3), both WALP and LAT peptides show a higher affinity for the DPPC rich Lo domain in presence of the gangliosides. This is in support of the hypothesized role of GM1 as helping proteins to sort into Lo domains.[11–13]

Taken together, our results underline the important role that gangliosides in general, and GM1 in particular, may have in the overall organization of the cell membrane. GM1 seems to have the remarkable combination of properties that (*i*) makes them readily partition into Lo domains, and (*ii*) allows them to bind to TM peptides. These features provide them with the ability to act as nano-shuttles for the sorting of membrane embedded proteins into ordered membrane regions. Although we did not attempt to further unravel the driving forces for the GM1–peptide association, it appears that the large oligosaccharide head group plays an important role in this process—the membrane embedded WALP or LAT peptides leave room for the GM1 head group, if it were, to embrace the peptides. The organization of the GM1 induced nano-domain is illustrated in Fig. 7 by a snapshot from the simulation involving LAT peptides, showing the ganglioside coat around the TM helices. Whether or not a similar embracement can take place with larger proteins remains to be seen. It would also be interesting to investigate what effect a higher concentration of cholesterol has on the GM1 conformation in our model, and consequently on the binding of GM1 to membrane proteins, since it is known that cholesterol effects both the head group orientation and binding of soluble proteins.[60] However, this is outside the scope of the current study.

3.4 Limitations

For a proper interpretation of the results described in the preceding sections, it is important to discuss some of the limitations of our model. An important simplification is the fixation of secondary protein structure in the Martini protein model.[26] Due to the limited resolution of the protein backbone, realistic folding is out of reach and the secondary structure is restrained to that of the initial (*e.g.* crystal) structure. In the current application, this limitation might have affected the partitioning behaviour of the Ras proteins, which are anchored in the membrane *via* a flexible loop (the HVR, see Fig. 1). As the structure of this loop is not resolved we modelled it as a random coil, a questionable assumption. Besides, activation of the Ras protein may affect the secondary structure of this loop *in vivo*, but this we obviously cannot take into account. A similar restriction applies to the conformational flexibility of the GM1 oligosaccharide head group, which was restrained using an elastic network as explained in the supporting material. Preliminary results with an improved model

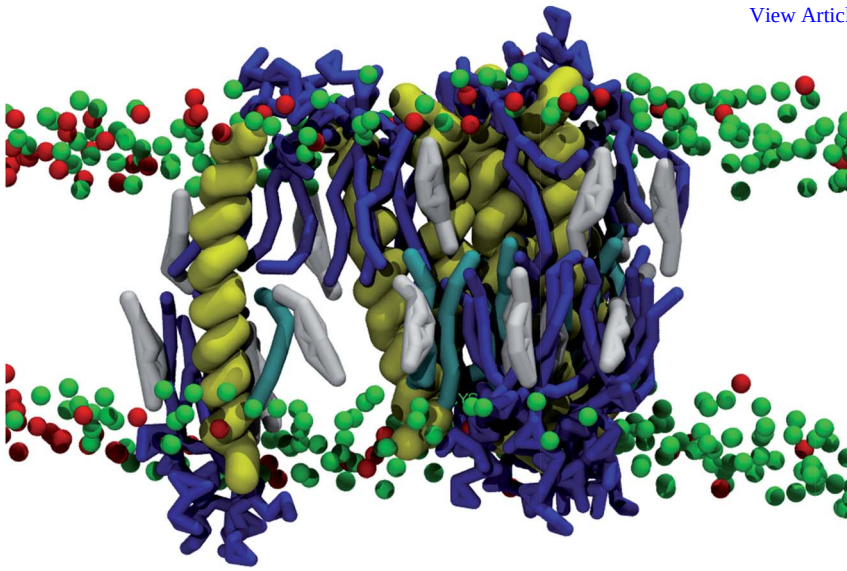

Fig. 7 Molecular view of a raft-embedded nano-domain composed of gangliosides and LAT peptides. The snapshot shows a cluster of GM1 lipid (blue) and LAT peptides (yellow) with lipid anchors (cyan). Cholesterol molecules are shown in white. Of the DPPC and DLiPC lipids only the head groups are shown as green and red spheres, respectively.

of GM1, lacking an elastic network, show similar behavior. A further point of concern is the oligomerization we observe in case of the soluble proteins. Both Ras variants as well as the Hedgehog protein form linear aggregates that do not dissociate once formed. Although it is not clear from experimental data to what extent this clustering is realistic or not, it could be that the Martini model overestimates the binding affinity of soluble proteins. We recently showed that, on the level of individual amino acids, dimerization free energies of amino acid side chain pairs are well reproduced in comparison to atomistic data.[61] This would point to a collective effect arising between protein surfaces, possibly related to the dewetting of these surfaces by the CG water beads that are large compared to real water molecules (recalling that a CG water represents four real waters). Eventually, some of the results obtained here with the Martini model will have to be checked using atomistic models. Considering the three orders of magnitude speed-up of the CG model with respect to atomistic models, this is not yet possible due to computational limitations.

Another point worth discussing is our choice of membrane composition. We face two challenges: on the one hand we need a lipid mixture that undergoes strong enough phase separation to result in well distinguishable Lo and Ld domains on a length scale of $\sim$20 nm, the size of our simulation box. On the other hand we like to resemble the *in vivo* situation, which is closer to a near critical mixture characterized by fluctuating nano-domains rather than macroscopic phase separation.[2] The mixture of DPPC, DLiPC, and cholesterol at approximately 6 : 4 : 1 ratio used in this study fulfils these criteria—it is weakly phase separating resulting in distinct regions of Lo and Ld domains that are yet very dynamic and able to rearrange on the sub-microsecond time scale of our simulations. Still, the partitioning of lipid anchored proteins in such a mixture will be determined by the difference in chemical potential of these proteins in either the Lo or Ld phase, and this may depend critically on the composition of the respective domains. Systematic exploration of the partitioning behaviour of membrane proteins as a function of lipid composition is

clearly needed. To arrive at a more realistic description of compartmentalization in real membranes, a few more steps are required. The current model membranes are yet lacking the complex composition of *in vivo* plasma membranes. Some important differences are: (*i*) the asymmetry between the inner and outer monolayers is lacking, (*ii*) the use of DPPC as saturated lipid, instead of sphingomyelin found *in vivo*, (*iii*) the lack of minor membrane constituents, both lipids and proteins, and (*iv*) the lack of cytoskeleton interacting with the membrane. We are currently working on a complex, more realistic lipid–protein mixture to further study the organizational principles in cell membranes.

4 Conclusion

We have simulated the partitioning behaviour of several membrane constituents that are thought to be involved, or even play an important role, in the domain formation of the plasma membrane. We find that peripheral Ras proteins partition to the Lo or Ld phase depending on the type of anchor. Double palmitoylated H-Ras prefers the Lo phase, whereas single palmitoylated N-Ras resides at the domain boundaries. De-palmitoylated H-Ras, with only a farnesyl anchor remaining, partitions into the Ld phase. Our results for the Hedgehog protein show that a single cholesterol anchor is sufficient to bring the protein in the Lo phase. Transmembrane peptides partition to the Ld phase, but saturated lipid anchors drive them toward the Lo–Ld domain boundary. Addition of GM1 ganglioside lipids does decrease the preference of the transmembrane peptides for the Ld even further. Interestingly, we find that the GM1 and peptides are capable of forming small nano-domains with high affinity for the Lo phase. This indicates that GM1 might play an important role in the recruiting of transmembrane proteins to membrane rafts.

References

1 L. A. Bagatolli, J. H. Ipsen, A. C. Simonsen and O. G. Mouritsen, *Prog. Lipid Res.*, 2010, **49**, 378–389.
2 D. Lingwood and K. Simons, *Science*, 2010, **327**, 46–50.
3 G. van Meer, D. R. Voelker and G. W. Feigenson, *Nat. Rev. Mol. Cell Biol.*, 2008, **9**, 112–124.
4 K. Simons and D. Toomre, *Nat. Rev. Mol. Cell Biol.*, 2000, **1**, 31–39.
5 T. Baumgart, A. T. Hammond, P. Sengupta, S. T. Hess, D. A. Holowka, B. A. Baird and W. W. Webb, *Proc. Natl. Acad. Sci. U. S. A.*, 2007, **104**, 3165–3170.
6 N. Kahya, D. Scherfeld, K. Bacia, B. Poolman and P. Schwille, *J. Biol. Chem.*, 2003, **278**, 28109–28115.
7 S. L. Veatch, I. V. Polozov, K. Gawrisch and S. L. Keller, *Biophys. J.*, 2004, **86**, 2910–2922.
8 I. Levental, M. Grzybek and K. Simons, *Biochemistry*, 2010, **49**, 6305–6316.
9 F. X. Contreras, A. M. Ernst, P. Haberkant, P. Björkholm, E. Lindahl, B. Gönen, C. Tischer, A. Elofsson, G. Von Heijne, C. Thiele, R. Pepperkok, F. Wieland and B. Brügger, *Nature*, 2012, **481**, 525–529.
10 B. Thaa, I. Levental, A. Herrmann and M. Veit, *Biochem. J.*, 2011, **437**, 389–397.
11 C. Yuan and L. J. Johnston, *Biophys. J.*, 2000, **79**, 2768–2781.
12 A. Prinetti, N. Loberto, V. Chigorno and S. Sonnino, *Biochim. Biophys. Acta, Biomembr.*, 2009, **1788**, 184–193.
13 B. Westerlund and J. P. Slotte, *Biochim. Biophys. Acta, Biomembr.*, 2009, **1788**, 194–201.
14 S. Sonnino, L. Mauri, V. Chigorno and A. Prinetti, *Glycobiology*, 2006, **17**, 1R.
15 R. K. Yu, Y. T. Tsai, T. Ariga and M. Yanagisawa, *J. Oleo Sci.*, 2001, **60**, 537–544.
16 N. Ichikawa, K. Iwabuchi, H. Kurihara, K. Ishii, T. Kobayashi, T. Sasaki, N. Hattori, Y. Mizuno, K. Hozumi, Y. Yamada and E. Arikawa-Hirasawa, *J. Cell Sci.*, 2009, **122**, 289–299.
17 R. G. Zhang, D. L. Scott, M. L. Westbrook, S. Nance, B. D. Spangler, G. G. Shipley and E. M. Westbrook, *J. Mol. Biol.*, 1995, **251**, 563–573.
18 T. Mitsuda, K. Furukawa, S. Fukumoto, H. Miyazaki, T. Urano and K. Furukawa, *J. Biol. Chem.*, 2002, **277**, 11239–11246.
19 N. Kawashima, S. J. Yoon, K. Itoh and K. I. Nakayama, *J. Biol. Chem.*, 2009, **284**, 6147–6155.

20 H. J. Kaiser, D. Lingwood, I. Levental, J. L. Sampaio, L. Kalvodova, L. Rajendran and K. Simons, *Proc. Natl. Acad. Sci. U. S. A.*, 2009, **106**, 16645–16650.
21 B. J. Reynwar and M. Deserno, *Biointerphases*, 2008, **3**, FA117–FA124.
22 F. J. M. de Meyer, M. Venturoli and B. Smit, *Biophys. J.*, 2008, **95**, 1851–1865.
23 X. Periole, T. Huber, S. J. Marrink and T. P. Sakmar, *J. Am. Chem. Soc.*, 2007, **129**, 10126–10132.
24 D. L. Parton, J. W. Klingelhoefer and M. S. P. Sansom, *Biophys. J.*, 2011, **101**, 691–699.
25 S. J. Marrink, H. J. Risselada, S. Yefimov, D. P. Tieleman and A. H. de Vries, *J. Phys. Chem. B*, 2007, **111**, 7812–7824.
26 L. Monticelli, S. K. Kandasamy, X. Periole, R. G. Larson, D. P. Tieleman and S. J. Marrink, *J. Chem. Theory Comput.*, 2008, **4**, 819–834.
27 L. V. Schäfer, D. H. de Jong, A. Holt, A. J. Rzepiela, A. H. de Vries, B. Poolman, J. A. Killian and S. J. Marrink, *Proc. Natl. Acad. Sci. U. S. A.*, 2011, **108**, 1343–1348.
28 J. Domanski, S. J. Marrink and L. V. Schäfer, *Biochim. Biophys. Acta, Biomembr.*, 2011, **1818**, 984–994.
29 G. von Heijne, *EMBO J.*, 1986, **5**, 3021–3027.
30 E. Sparr, W. L. Ash, P. V. Nazarov, D. T. S. Rijkers, M. A. Hemminga, D. P. Tieleman and J. A. Killian, *J. Biol. Chem.*, 2005, **280**, 39324–39331.
31 H. J. Risselada and S. J. Marrink, *Proc. Natl. Acad. Sci. U. S. A.*, 2008, **105**, 17367–17372.
32 U. Krengel, *Thesis, Heidelberg*, 1991.
33 A. Wernimont and A. Edwards, *PLoS One*, 2009, **4**, e5094.
34 The PyMOL Molecular Graphics System, Version 1.2r1, Schrödinger, LLC.
35 D. H. de Jong, W. F. D. Bennet, G. Singh, C. Arnarez, T. A. Wassenaar, L. V. Schäfer, X. Periole, D. P. Tieleman and S. J. Marrink, *J. Chem. Theory Comput., In preparation*, 2012.
36 X. Periole, M. Cavalli, S. J. Marrink and M. A. Ceruso, *J. Chem. Theory Comput.*, 2009, **5**, 2531–2543.
37 T. M. Hall, J. A. Porter, P. A. Beachy and D. J. Leahy, *Nature*, 1995, **378**, 212–216.
38 J. A. Killian, I. Salemink, M. R. R. de Planque, G. Lindblom, R. E. Koeppe II and D. V. Greathous, *Biochemistry*, 1996, **35**, 1037–1045.
39 B. Y. Duyl, D. T. S. Rijkers, B. de Kruijff and J. A. Killian, *FEBS Lett.*, 2002, **523**, 79–84.
40 C. A. Lopez, A. Rzepiela, A. H. de Vries, L. Dijkhuizen, P. H. Hünenberger and S. J. Marrink, *J. Chem. Theory Comput.*, 2009, **5**, 3195–3210.
41 B. Hess, C. Kutzner, D. van der Spoel and E. Lindahl, *J. Chem. Theory Comput.*, 2008, **4**, 435–447.
42 S. Ramadurai, A. Holt, L. V. Schäfer, V. V. Krasnikov, D. T. S. Rijkers, S. J. Marrink, J. A. Killian and B. Poolman, *Biophys. J.*, 2010, **99**, 1447–1454.
43 K. Wennerberg, K. L. Rossman, and C. J. Der, J. Cell. Sci, **118**, pp. 843–846.
44 I. A. Prior and J. F. Hancock, *J. Cell. Sci.*, 2001, **114**, 1603–1608.
45 C. Nicolini, J. Baranski, S. Schlummer, J. Palomo, M. Lumbierres-Burgues, M. Kahms, J. Kuhlmann, S. Sanchez, E. Gratton, H. Waldmann and R. Winter, *J. Am. Chem. Soc.*, 2006, **128**, 192–201.
46 K. Weise, S. Kapoor, C. Denter, J. Nikolaus, N. Opitz, S. Koch, G. Triola, A. Herrmann, H. Waldmann and R. Winter, *J. Am. Chem. Soc.*, 2011, **133**, 880–887.
47 L. Janosi, Z. Li, J. F. Hancock and A. A. Gorfe, *Proc. Natl. Acad. Sci. U. S. A.*, 2011, **109**, 8097–8102.
48 I. A. Prior, A. Harding, J. Yan, J. Sluimer, R. G. Parton and J. F. Hancock, *Nat. Cell Biol.*, 2001, **3**, 368–375.
49 H. Niv, O. Gutman, Y. Kloog and Y. I. Henis, *J. Cell Biol.*, 2002, **157**, 865–872.
50 A. A. Gorfe, M. Hanzal-Bayer, D. Abankwa, J. F. Hancock and J. A. McCammon, *J. Med. Chem.*, 2007, **50**, 674–684.
51 R. Thapar, J. G. Williams and S. L. Campbell, *J. Mol. Biol.*, 2004, **343**, 1391–1408.
52 J. A. Porter, K. E. Young and P. A. Beachy, *Science*, 1996, **274**, 255–259.
53 R. B. Pepinsky, C. Zeng, D. Wen, P. Rayhorn, D. P. Baker, K. P. Williams, S. A. Bixler, C. M. Ambrose, E. A. Garber, K. Miatkowski, F. R. Taylor, E. A. Wang and A. Galdes, *J. Biol. Chem.*, 1998, **273**, 14037–14045.
54 A. Rietveld, S. Neutz, K. Simons and S. Eaton, *J. Biol. Chem.*, 1999, **274**, 12049–12054.
55 M. R. R. de Planque and J. A. Killian, *Mol. Membr. Biol.*, 2003, **20**, 271–284.
56 H. Shogomori, A. T. Hammond, A. G. Ostermeyer-Fay, D. J. Barr, G. W. Feigenson, E. London and D. A. Brown, *J. Biol. Chem.*, 2005, **280**, 18931–18942.
57 I. Levental, D. Lingwood, M. Gryzbek, Ü. Coskun and K. Simons, *Proc. Natl. Acad. Sci. U. S. A.*, 2010, **107**, 22050–22054.
58 S. Trabelsi, S. Zhang, T. R. Lee and D. K. Schwartz, *Phys. Rev. Lett.*, 2008, **100**, 037802.
59 A. Ferraretto, M. Pitto, P. Palestini and M. Masserini, *Biochemistry*, 1997, **36**, 9232–9236.
60 D. Lingwood, B. Binnington, T. Rog, I. Vattulainen, M. Grzybek, U. Coskun, C. A. Lingwood and K. Simons, *Nat. Chem. Biol.*, 2011, **7**, 260–262.
61 D. H. de Jong, X. Periole and S. J. Marrink, *J. Chem. Theory Comput.*, 2012, **8**, 1003–1014.